Remote Sensing of Environment 260 (2021) 112466

Contents lists available at ScienceDirect

Remote Sensing of Environment

journal homepage: www.elsevier.com/locate/rse

Using time series of MODIS land surface phenology to model temperature and photoperiod controls on spring greenup in North American deciduous forests

Minkyu Moon [a,*], Bijan Seyednasrollah [b,c], Andrew D. Richardson [b,c], Mark A. Friedl [a]

[a] Department of Earth and Environment, Boston University, USA
[b] School of Informatics, Computing, and Cyber Systems, Northern Arizona University, USA
[c] Center for Ecosystem Science and Society, Northern Arizona University, USA

ARTICLE INFO

Keywords:
Spring phenology
Climate change
Deciduous forests
Photoperiod
Temperature sensitivity
Bayesian
Hierarchical modeling
MODIS
Land surface phenology

ABSTRACT

The timing of leaf emergence in temperate and boreal forests is changing, which has profound implications for a wide array of ecosystem processes and services. Spring phenology models, which have been widely used to predict the timing of leaf emergence, generally assume that a combination of photoperiod and thermal forcing control when leaves emerge. However, the exact nature and magnitude of how photoperiod and temperature individually and jointly control leaf emergence is the subject of ongoing debate. Here we use a continuous development model in combination with time series of land surface phenology measurements from MODIS to quantify the relative importance of photoperiod and thermal forcing in controlling the timing of canopy greenup in eastern temperate and boreal forests of North America. The model accurately predicts biogeographic and interannual variation in the timing of greenup across the study region (median RMSE = 4.6 days, median bias = 0.30 days). Results reveal strong biogeographic variation in the period prior to greenup when temperature and photoperiod influence greenup that covaries with the importance of photoperiod versus thermal controls. Photoperiod control on leaf emergence is dominant in warmer climates, but exerts only modest influence on the timing of leaf emergence in colder climates. Results from models estimated using ground-based observations of cloned lilac are consistent with those from remote sensing, which supports the realism of remote sensing-based models. Overall, results from this study suggest that apparent changes in the sensitivity of trees to temperature are modest and reflect a trade-off between decreased sensitivity to temperature and increased photoperiod control, and identify a transition in the relative importance of temperature versus photoperiod near the 10 °C isotherm in mean annual temperature. This suggests that the timing of leaf emergence will continue to move earlier as the climate warms, and that the magnitude of change will be more pronounced in colder regions with mean annual temperatures below 10 °C.

1. Introduction

There is overwhelming evidence that leaf emergence is occurring earlier in temperate and boreal forests (Menzel et al., 2006; Schwartz et al., 2006). However, a number of recent papers have concluded that the sensitivity of leaf emergence to changes in temperature has decreased in recent decades (Fu et al., 2015; Piao et al., 2017) and that the period when trees are sensitive to thermal forcing is becoming shorter (Fu et al., 2019; Güsewell et al., 2017; Wenden et al., 2020). These results complicate interpretation of observed trends and exacerbate challenges involved in forecasting how the phenology of trees will change in the future. These challenges are further complicated by fundamental issues in the way that the sensitivity of phenological events to temperature is generally quantified (Keenan et al., 2019). Because changes in phenology impact important ecosystem functions (Keenan et al., 2014; Richardson et al., 2013), understanding how changes in climate affect phenology is critical to forecasting how ecosystems will respond to future climate change (Peñuelas et al., 2009; Piao et al., 2019).

To address this, a variety of recent studies have focused on improving understanding of bioclimatic controls on plant phenology (Liu et al., 2017; Zohner et al., 2016). Results from both lab- and field-based

* Corresponding author at: 685 Commonwealth Avenue, Boston, MA 02215, USA.
E-mail address: moon.minkyu@gmail.com (M. Moon).

https://doi.org/10.1016/j.rse.2021.112466
Received 3 November 2020; Received in revised form 7 April 2021; Accepted 17 April 2021
Available online 22 April 2021

experimental studies have provided insights (Montgomery et al., 2020; Richardson et al., 2018a), but are limited by the fact that phenological behavior in controlled laboratory- and field-based warming experiments differs from behavior observed in natural ecosystems (Clark et al., 2014a; Wolkovich et al., 2012). Further, the manner in which environmental conditions are perturbed in such experiments (e.g., 2 °C warming) is not representative of climate changes expected in the future, which are predicted to occur gradually, but with large year-to-year variability (Schewe et al., 2019; Walther et al., 2002). These issues are compounded by the fact that the geographic sampling of data sets used in these studies is often limited and does not reflect the full biogeographic range of species examined (Richardson et al., 2013). Hence, geographic variation in the relative importance of different climate drivers on phenology, both within and across plant communities, is not well understood (Piao et al., 2019).

One widely used strategy for investigating the response of plant phenology to climate change is to calibrate mechanistic models using weather data in combination with long-term records of phenology collected on the ground (Basler, 2016; Fu et al., 2019) or from remote sensing (Liu et al., 2017; Melaas et al., 2018). In addition to thermal controls, photoperiod is widely assumed to control the timing of leaf emergence by regulating the entrance of ecodormancy, triggering thermal forcing to stimulate bud swelling and leaf emergence (Chuine et al., 2016; Jackson, 2009; Körner and Basler, 2010). Hence, many models include explicit representation of photoperiod (e.g., Blümel and Chmielewski, 2012; Masle et al., 1989; Basler, 2016; Migliavacca et al., 2012). To capture the role of thermal forcing, mechanistic models generally use aggregated bioclimatic variables such as growing degree days or winter chilling as their primary inputs. However, Clark et al. (2014a) have suggested that the use of such aggregated quantities is problematic because values for prescribed variables required by these models (e.g., start date of forcing accumulation) are not identifiable.

In recent years, data-driven models based on state-space representations of phenological processes have been developed that overcome many of the weaknesses of both mechanistic and experimental approaches (e.g., Clark et al., 2014b; Qiu et al., 2020; Senf et al., 2017; Seyednasrollah et al., 2018). By modeling phenological dynamics directly from data, these models avoid issues arising from misspecification of functional relationships between forcing variables and processes that regulate phenological development (Clark et al., 2014b). Building on this approach, here we use a data-driven spring onset model in combination with gridded weather data and time series of ground-based and remotely sensed observations of spring greenup dates to explore biogeographic patterns in photoperiod and thermal controls on the timing of spring greenup. Specifically, we use this model to: (1) quantify the relative importance of thermal forcing, photoperiod, and winter chilling in controlling spring greenup; (2) identify the pre-season period when plants are sensitive to bioclimatic controls; and (3) characterize how covariance among thermal forcing, photoperiod, and the length of the pre-season period control the biogeography of spring greenup in deciduous forests of eastern temperate and boreal North America.

2. Methods

2.1. Study region

The study region includes the Northern Forests and Eastern Temperate Forest ecoregions included in Level I of the US EPA Ecoregions of North America (Fig. A1). To distinguish deciduous forests from evergreen forests and other land cover types within the study area, the 500 m Collection 6 MODIS Land Cover Type product was used. This product provides annual land cover maps based on machine learning that are post-processed using a multi-temporal state-space modeling framework that reduces spurious land cover change introduced by classification uncertainty in individual years (Abercrombie and Friedl, 2016; Sulla-Menashe et al., 2019).

The continuous development spring onset model (Section 2.3) is estimated on an equal-area grid, where each grid cell is 4.67 km × 4.67 km (10 × 10 MODIS pixels; ~22 km^2). In each grid cell, only pixels labeled as deciduous broadleaf or mixed forests throughout the entire study period from 2001 to 2017 were included in the analysis. To ensure analyses were based on grid cells dominated by deciduous forest cover, we excluded model grid cells where the fraction of MODIS pixels labeled as deciduous broadleaf or mixed forests was less than 50% (Fig. A1).

2.2. Spring greenup and meteorological data

To identify the timing of springtime leaf emergence from 2001 to 2017, we used the Collection 6 MODIS Land Cover Dynamics product (MCD12Q2; Gray et al., 2019). This product uses time series of the two-band Enhanced Vegetation Index (EVI2) to identify the timing of six key phenophase transition dates during each growing season in each 500-m MODIS pixel. Numerous studies have reported that this product provides a reliable measure of vegetation phenology (Moon et al., 2019; Richardson et al., 2018b) and seasonal changes in ecological function and surface biophysical characteristics (Melaas et al., 2013; Moon et al., 2020). For this analysis, we use the MCD12Q2 'greenup' metric, which is defined by the Land Cover Dynamics product as the day of year (DOY) during the greenup phase in spring when the EVI2 time series at each pixel crosses 15% of its seasonal amplitude (Gray et al., 2019).

To provide the meteorological data required for model estimation, we used the Version 3 Daymet dataset for North America (Thornton et al., 2017) (https://daymet.ornl.gov). This data set uses digital elevation data in association with a land-water mask and meteorological observations collected at ground-based stations to create gridded time series of surface meteorological fields at daily time step and 1 km spatial resolution for the period 1980 to present. For this work, we used daily maximum and minimum 2-m air temperatures from 2000 to 2017 along with day-length, resampled to 500 m and co-registered to the MODIS data over all grid cells included in our analysis.

2.3. Continuous Development Spring Onset Model

To estimate the sensitivity of different climatological controls on springtime phenology, we developed a continuous development spring onset model (hereafter, CDSOM) based on a hierarchical Bayesian framework that predicts the timing of springtime greenup using three drivers: photoperiod, thermal forcing, and chilling units. The original form of this model was proposed by Clark et al. (2014b), who used the same general approach to show that because conventional process-based phenology models (e.g., Hufkens et al., 2018.) aggregate daily air temperature time series into cumulative sums or mean values for each year or season, they misrepresent how thermal forcing controls the timing of phenology.

Similar to Clark et al. (2014b), the CDSOM we use here tracks the continuous response of phenological development to variation in environmental controls at daily time step. To do this, the model uses a state-space framework that includes an unobservable latent state (h), which responds continuously to environmental controls and captures ecological responses to bioclimatic forcing:

$$h_{g,s,d+1} = h_{g,s,d} + \delta h_{g,s,d} \tag{1}$$

where $h_{g,\,s,\,d}$ is the latent state for grid cell g and sample (i.e., pixel) s on day d. In this framework, $\delta h_{g,\,s,\,d}$ is the increment in h from day d to day $d + 1$, which is estimated using:

$$\delta h_{g,s,d} = \begin{cases} \left(X_{g,s,d} \times \beta_g\right)\left(1 - h_{g,s,d}/h_{max}\right) \; for \; \delta h_{g,s,d} \geq 0 \\ 0 \; for \; \delta h_{g,s,d} < 0 \end{cases} \tag{2}$$

where $X_{g,\,s,\,d}$ is a matrix of predictor variables that includes the daily mean temperature ($T_{g,\,s,\,d}$), day-length (i.e., photoperiod; $L_{g,\,s,\,d}$), and

chilling units ($CU_{g,s}$; defined below) on each day, and where daily mean temperature is computed as the average of daily maximum and minimum temperatures from Daymet in each 500 m MODIS pixel. β_g is a vector of estimated model coefficients for each grid cell (g), and h_{max} is the final state value of h, which is prescribed to be 100. Note that: (1) even though a linear formulation is used to describe the relationship between model predictors and coefficients, the model accommodates nonlinear responses in phenological responses to environmental controls using an asymptotic limit for the latent state (i.e., $h_{g,s,d}/h_{max}$); and (2) the latent state increment is always non-negative.

To convert the continuous scale of the latent state (h) into a form that identifies discrete phenological events (i.e., the timing of spring greenup onset), a logit transformation is used:

$$logit\left(P_{g,s,d}\right) = \kappa + \lambda \times h_{g,s,d} \tag{3}$$

where $P_{g,s,d}$ is the probability that the onset occurs at sample pixel s in grid g on day d, and κ and λ are the intercept and slope of the transformation, respectively. Because greenup onset is defined to be a discrete event, $P_{g,s,d}$ follows a Bernoulli distribution:

$$Y_{g,s,d} \sim Bernoulli\left(P_{g,s,d}\right) \tag{4}$$

where $Y_{g,s,d}$ indicates whether or not greenup onset has occurred for sample s in grid g on day d.

Following convention, chilling units ($CU_{g,s}$) were defined as:

$$CU_{g,s} = \sum_{d=c_{g,0}}^{c_{g,s}} I\left(T_{g,s,d} < T_b\right) \tag{5}$$

Hence, $CU_{g,s}$ is defined as the number of days below prescribed threshold T_b during the period after the onset of dormancy until an unobserved date $c_{g,s}$ when the chilling requirement is satisfied. Previous studies have suggested that boreal and temperate tree species respond to air temperatures ranging from −5 to 10 °C as a threshold for chilling requirements (Hänninen et al., 2019). Here we used 0 °C because the study area covers a large range of climate conditions. Further, and more importantly, sensitivity analyses revealed that model results were not sensitive to variation in T_b (not shown), which is supported by results indicating that chilling control on the timing of greenup is minor (see Results).

2.4. CDSOM estimation

As we described above, the CDSOM was estimated using a regular grid, with each grid cell composed of 100 MODIS pixels. We excluded all pixels with more than one land cover type label between 2001 and 2017 (i.e., that nominally experienced change) and excluded all cells that were composed of less than 50% deciduous or mixed forests. Because the CDSOM is computationally expensive, we used a two-stage sampling approach to estimate the model for randomly selected grid cells in each of the 13 MODIS tiles that intersect the study region. In the first stage, we randomly sampled grid cells within each MODIS tile that met the criteria listed above. If less than 300 valid grid cells were available within a tile, we included all valid grid cells. If more than 300 grid cells were available in a tile, we randomly selected a sample of 300 cells. In the second stage, we randomly selected MODIS pixels located in each grid cell across time. To minimize the impact of spatial and temporal correlation, we used a sub-sample of 100 pixel-years (i.e., 100 unique greenup dates randomly selected across 17 years) to estimate a unique model for each cell. Each sample was selected from a total pool of between 850 and 1700 sample points (i.e., 50–100 pixels per year in each grid across 17 years).

For each year, December 1st of the previous year and DOY 250 (~Sept. 7) of the current year were used as the start and end dates of latent state development, respectively. Posterior sampling was performed using the "R2jags" package in R (Su and Yajima, 2015), with 10,000 iterations and 3000 burn-in periods. As a final step, to reduce noise in our results, we excluded grid cells where estimated model coefficients were outside 95% of the range of estimated model coefficients across all grid cells. This yielded a final data set consisting of 1685 grid cells with valid results.

Model results from a representative grid cell are shown in Fig. 1. Overall, predicted onset dates are well aligned with observed onset dates at this grid cell, with a root-mean-square error (RMSE) of 3.7 days across the time series (Fig. 1a). Because the input forcing data are normalized prior to model estimation (i.e., having a mean of 0 and a standard deviation of 1 for each of the input variables in each grid g and sample s), the posterior distributions for each model coefficient, which reflect the dependence of phenological development on each input variable, show differences that are independent of the magnitude or units of each input variable (Fig. 1b). Time series of the latent state generated by the model (Fig. 1c) provide information regarding the timing and duration of the pre-season period prior to greenup onset. This period has been previously described as "as the most temperature-sensitive period preceding the phenological event" (Güsewell et al., 2017) or "the period before leaf unfolding for which the partial correlation coefficient between leaf unfolding and air temperature is highest" (Fu et al., 2015). Here we define this period as corresponding to the time interval when phenological development is affected by bioclimatic forcing, and we use the CDSOM to identify the "pre-season period" as starting on the DOY when the latent state variable (h) starts to increase and ending on the DOY when greenup onset occurs (i.e., the period indicated by the arrow in Fig. 1c).

2.5. Quantifying the relative importance of bioclimatic forcing variables

To address our goal of quantifying the relative importance (and geographic variation thereof) among bioclimatic controls on the timing of springtime phenology, we compute a normalized index with values that range from −1 to +1 that captures this effect. Because each of the input variables in each grid g and sample s have been normalized to have a mean of 0 and a standard deviation of 1, model coefficients can be directly compared to assess the relative importance of each control variable. To quantify this, we calculated the relative importance (RI) of each control variable relative to each other variable using a normalized index computed from CDSOM model results. For example, to compute the relative importance of photoperiod versus thermal forcing in any given grid cell, we computed:

$$RI = \frac{\beta_T - \beta_L}{\beta_T + \beta_L} \tag{6}$$

where β_T and β_L are the average model coefficients for thermal forcing and photoperiod (respectively) during the pre-season period, which are estimated for each grid cell by the CDSOM.

2.6. CDSOM assessment and comparison with conventional phenology models

To provide a baseline comparison against previously developed and widely used springtime phenology models (hereafter, the 'conventional models'), we compared results from the CDSOM with four widely used process-based phenology models included in the "phenor" package in R (Hufkens et al., 2018). Specifically, we compared our results against the thermal time (TT) model, the photo-thermal time (PTT) model, the exponential photo-thermal time model (M1), and the alternating (AT) model, as described by Hufkens et al. (2018). These models are fundamentally different from the CDSOM in that they assume a linear relationship between spring thermal forcing and the rate of phenological development, and that spring onset occurs when accumulated forcing (after a prescribed start date) reaches a critical threshold (F^*). The TT model relies only on thermal forcing (daily air temperature in each

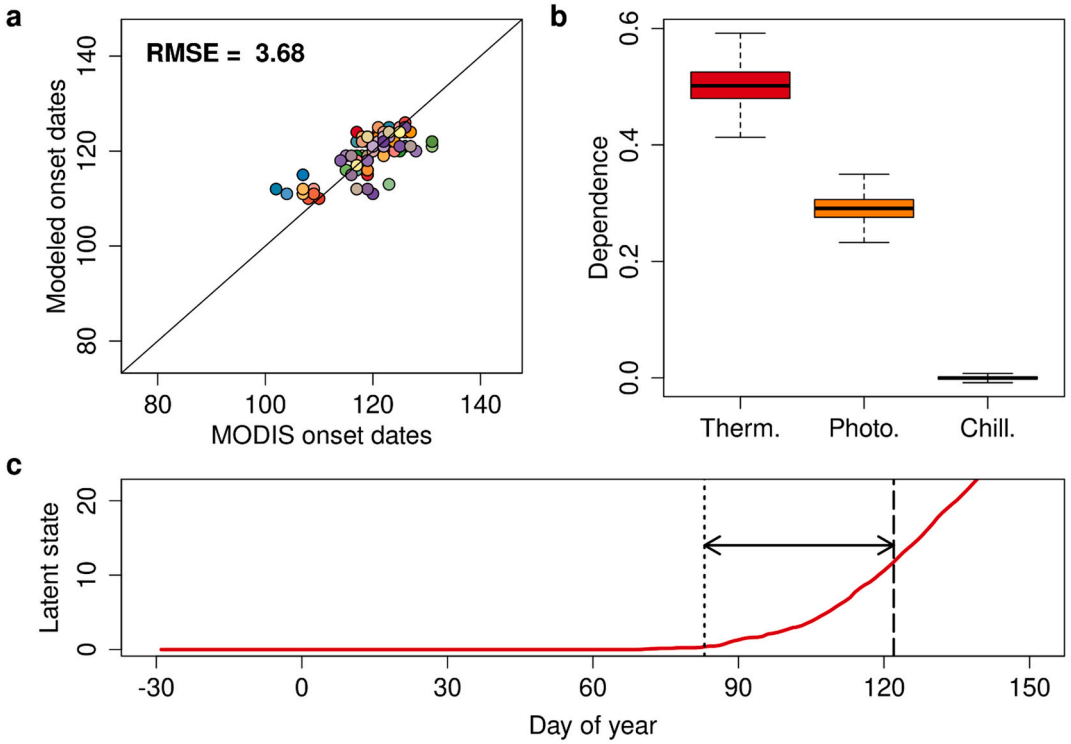

Fig. 1. Model results for a randomly selected grid cell. (a) Relationship between the greenup onset dates from MODIS and onset dates estimated by the model. (b) The distribution of model coefficients for each control variable (i.e., the relative dependence on each climate control; Therm.: thermal forcing; Photo.: photoperiod; Chill.: chilling units). (c) Time series of the latent state (red line) and the length of the pre-season (identified by the horizontal arrow). In panel (a), each dot (total $n = 100$) represents an individual pixel-year sampled from the grid cell comprised of 10 by 10 MODIS pixels across 17 years of the study period (i.e., 100 out of the total 1700 pixel-years). (For interpretation of the references to colour in this figure legend, the reader is referred to the web version of this article.)

MODIS pixel, $T_{g,\,s,\,d}$) with no additional inputs. In this model, the state of forcing (S_f) increases each day until F^* is reached, when leaves emerge (Chuine et al., 1999; Hunter and Lechowicz, 1992):

$$R(T_{g,s,d}) = \begin{cases} 0 \; for \; T_{g,s,d} \le T_b \\ T_{g,s,d} - T_b \; for \; T_{g,s,d} \ge T_b \end{cases} \tag{7}$$

$$S_f = \sum_{t_0}^{t} R(T_{g,s,d}) \tag{8}$$

where t_0 is the starte date. For consistency with the CDSOM, we set t_0 and T_b to December 1st and 0 °C, respectively. The PTT model includes day-length (i.e., photoperiod; $L_{g,\,s,\,d}$) as an additional factor that regulates the rate of thermal forcing (Črepinšek et al., 2006; Masle et al., 1989):

$$S_f = \sum_{t_0}^{t} R(T_{g,s,\mathrm{d}}) \times \frac{L_{g,s,d}}{24} \tag{9}$$

The exponential M1 model also includes photoperiod, but treats the relationship between photoperiod and S_f as an exponential (Blümel and Chmielewski, 2012):

$$S_f = \sum_{t_0}^{t} R(T_{g,s,d}) \times \left(\frac{L_{g,s,d}}{24}\right)^k \tag{10}$$

where k is an empirically estimated constant. Finally, the AT model includes the number of days when the daily mean temperature falls below T_b (i.e., the number of chilling days; NCD), and treats NCD as an exponential function that reduces the thermal forcing accumulation required for spring onset to occur (Cannell and Smith, 1983):

$$F^* = a + b \times exp[c \times \mathrm{NCD}(t)\,] \tag{12}$$

where a, b, and c are empirically estimated constants, and NCD(t) is defined as the number of chilling days since December 1st. A table summarizing the variables and main characteristics of the CDSOM and conventional models is provided as an appendix (Table A1).

For this analysis, we assessed model performance for both the CDSOM and the conventional models in two ways. First, we assessed results from model-based predictions for the timing of spring greenup based on all available years (from 2001 to 2017). Second, to provide a more robust assessment of model performance, we held out two years (2010 and 2012) with anomalously warm springs in much of the study region (Friedl et al., 2014), and evaluated model performance for each of these years. In this way, we were able to assess not only how well the models performed under average conditions, but also how well they performed under unusual springtime weather conditions that were not represented in the data used to estimate the models.

2.7. CDSOM estimation using ground-based observations

As a final element of our analysis, to complement model results based on remotely sensed greenup dates and to provide an independent basis for assessing the realism and robustness of our results, we estimated the CDSOM using time series of leaf unfolding dates for cloned lilac (*Syringa x chinensis* 'Red Rothomagensis') (Rosemartin et al., 2015). By applying the model to data from cloned plants, genetic variability is eliminated, and which allows us to investigate how differences in the timing of leaf unfolding between different individuals are caused by differences in local environmental controls. Unlike our approach using MODIS spring greenup dates, the model is estimated by pooling site-years across the region because the number of lilac leaf-out dates for each location is too small to accurately estimate models for each site. The dataset includes 254 leaf unfolding dates from 60 locations across the study region, spanning the period from 2001 to 2008 (Fig. A1). For reasons we explain

below, we stratified the dataset into 'warm' versus 'cold' sites based on whether the mean annual temperature at each site is above or below 10 °C. Based on this stratification, the model was applied to 182 and 72 leaf unfolding dates for the colder and warmer regions, respectively.

3. Results

The CDSOM accurately predicts biogeographic and interannual variation in the timing of springtime greenup across the study region. The median RMSE between predicted and observed spring greenup dates was 4.6 days (Fig. 2), which is roughly equivalent to the uncertainty in spring greenup dates estimated from MODIS (Moon et al., 2019). Inspection of results from the conventional spring onset models show that median RMSEs were ~ 20% larger (~5.5 days vs. 4.6 days) relative to those obtained from the CDSOM (Fig. 2b). Further, RMSEs for years with anomalous springs (2010 and 2012) were unchanged for the CDSOM, but increased by roughly 2 days for conventional models when 2010 and 2012 were excluded during model estimation (Fig. 3). For completeness, Fig. A2 shows the relationship between anomalies in MODIS greenup dates and anomalies in predicted onset set dates, and demonstrates that the CDSOM outperforms the conventional models in capturing year-to-year variations in spring onset dates. These results suggest that the CDSOM not only provides more accurate predictions of greenup relative to predictions from conventional phenology models, but that the CDSOM more effectively captures the impact of geographic and year-to-year variation in bioclimatic controls. More generally, the accuracy of CDSOM results indicates that the model realistically captures the nature and magnitude of ecophysiological responses to interannual and biogeographic variation in climate controls that regulate the timing of greenup.

The dependence of spring greenup on thermal forcing estimated by the CDSOM is higher in Northern Forests than in Eastern Temperate forests (Fig. 4), but overall differences, while statistically significant, are modest (Fig. 4d). In contrast, dependence on photoperiod control exhibits systematic geographic variation across the study domain, with large differences between each ecoregion. Eastern Temperate Forests, which are warmer, show substantially higher dependence on photoperiod relative to the Northern Forests ecoregion, which is much cooler (Fig. 4b and d). This difference is especially pronounced in Eastern Canada where dependence on photoperiod is low, versus the Southern United States, where photoperiod dependence is high. Dependence of spring onset on chilling units is uniformly low throughout the study region, which indicates that the influence of chilling control, relative to photoperiod and thermal forcing, is effectively negligible (Fig. 4c and d).

Geographic patterns in the *RI* of photoperiod versus thermal forcing indicates that photoperiod exerts proportionally more control on the timing of spring greenup in warmer regions, while thermal forcing exerts proportionally more control in colder regions (Fig. 5a). By plotting the *RI* in climate space (i.e., as a function of mean annual temperature and precipitation) (Fig. 5b), the pattern becomes even more clear. In regions where mean annual temperature is above ~10 °C, photoperiod exerts stronger control on the timing of spring greenup than thermal forcing. Conversely, in regions where mean annual temperature is less than ~10 °C, thermal forcing is more important. *RI* values near the 10 °C isotherm in mean annual temperature are generally close to zero, indicating equal influence of thermal forcing and photoperiod (plotted as purple points in Fig. 5). These results suggest that the 10 °C isotherm in mean annual temperature identifies a transition zone between regions where thermal forcing versus photoperiod is more dominant.

Results from applying CDSOM to ground-based observations of leaf unfolding dates for cloned lilac reveal that even though the individual lilac plants are genetically identical, the relative dependence of leaf unfolding dates on thermal forcing versus photoperiod depends on local bioclimatic conditions (Fig. 6). Consistent with previous studies (Basler and Körner, 2012; Schwartz et al., 2006), model coefficients and *RI* values indicate that leaf unfolding in cloned lilac depends more strongly on thermal forcing than on photoperiod, irrespective of location. However, thermal control is stronger in colder regions and *RI* values are significantly smaller (i.e., thermal control is less dominant) in warm sites than in cold sites. In addition, comparison of cloned lilac data against greenup dates from MODIS for the same location show that MODIS greenup dates are biased late relative to lilac unfolding dates (Fig. A3), especially in warmer areas with earlier greenup dates, which

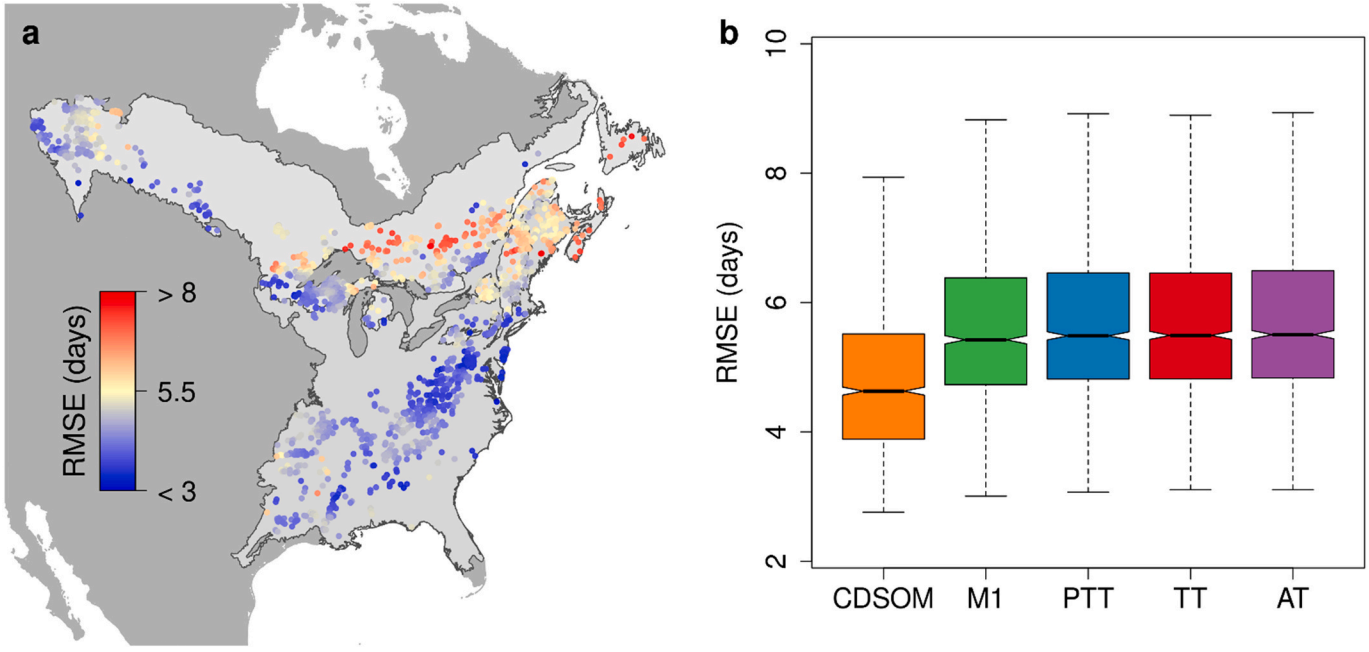

Fig. 2. Continuous Development Spring Onset Model (CDSOM) performance. (a) Geographic variation in model root-mean-square error (RMSE) between greenup onset dates observed from MODIS and onset dates predicted by the CDSOM model. (b) Boxplots showing the distribution of RMSEs for the CDSOM model and four widely used conventional spring greenup models. M1: The exponential photo-thermal time model; PTT: The photo-thermal time model; TT: The thermal time model; AT: The alternating model. In panel (b), boxplots are presented in increasing order of magnitude with respect to mean RMSE.

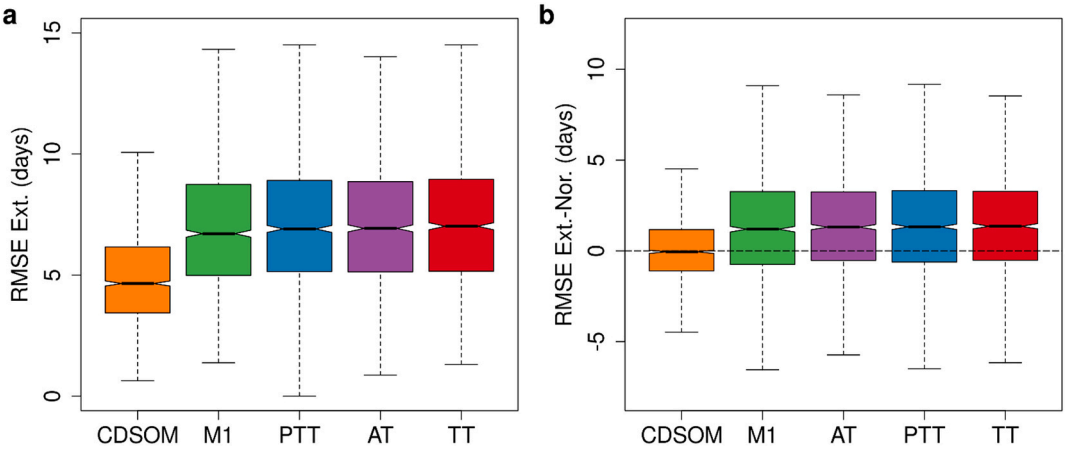

Fig. 3. RMSE results across models for anomalous years. (a) Boxplots of RMSEs for each model for 2010 and 2012. (b) Boxplots showing increase in RMSEs for model predictions for all years versus anomalous years (i.e., RMSEs for 2010 and 2012 – RMSEs for 2001–2017) at each grid cell. CDSOM: continuous development spring onset model; M1: The exponential photo-thermal time model; PTT: The photo-thermal time model; TT: The thermal time model; AT: The alternating model. Boxplots are presented in increasing order of magnitude with respect to mean RMSE.

supports the conclusion that lilacs are sensitive to temperature.

Finally, results from the CDSOM reveal patterns of covariance among pre-season period length, photoperiod, and thermal forcing that jointly control the timing of greenup that are not captured in conventional models. In particular, geographic variation in the pre-season period is strongly and negatively correlated with geographic variation in the relative importance of photoperiod on spring greenup. Fig. 7b shows that this relationship follows a power law, where photoperiod control decreases ($R^2 = 0.70$, $p < 0.001$) as the length of the pre-season period increases. Fig. 7b also reveals modest heteroscedasticity in the relationship between pre-season period length and photoperiod control, which reflects the fact that spring greenup in locations with cooler mean annual temperatures and longer pre-seasons have lower dependence on photoperiod and higher dependence on thermal forcing (Fig. 5). In contrast, the relationship between pre-season period and dependence on thermal forcing is statistically significant, but much weaker ($R^2 = 0.13$; Fig. A4).

4. Discussion

We assessed the relative importance of photoperiod, chilling, and thermal forcing in controlling the timing of leaf emergence in Eastern Temperate and Boreal Forest ecoregions of North America. To do this, we used a hierarchical Bayesian model in combination with time series of land surface phenology measurements from remote sensing. The former provides a data-driven framework for investigating how different bioclimatic controls influence the timing of leaf emergence (Clark et al., 2014b; Seyednasrollah et al., 2020); the latter provides a robust and repeatable means of measuring and monitoring phenological dynamics over large areas (Bolton et al., 2020; Zhang et al., 2018).

The core hypotheses that motivate this research include two main elements. First, the ecophysiological processes that control leaf emergence respond continuously to variation in environmental controls throughout pre-season period prior to greenup in a manner that is not represented in conventional models (Clark et al., 2014b). Second, rather than simply acting as a cue for entering ecodormancy, photoperiod exerts continuous control on the timing of greenup during the pre-season period. The results presented in this study suggest that both hypotheses are supported. The preseason period, which corresponds to the period when the CDSOM latent state variable (h) responds to bioclimatic forcing (Fig. 1c), ranges from roughly 2–12 weeks over the study domain (Fig. 7a). Throughout this period, changes in h reflect the net effect of daily changes thermal and photoperiod controls. By estimating the model in a spatially explicit fashion over a large geographic and climatic range, CDSOM results provide an empirical basis for quantifying not only how thermal forcing and photoperiod individually and jointly influence the timing of greenup, but more generally, how the length of the preseason period and relative importance of photoperiod versus thermal forcing vary over the study domain.

Conventional models calibrated using long-term observations of phenological events such as those used in this study have been widely used to simulate and forecast phenological events for decades (Chuine and Régnière, 2017). Like the CDSOM, these models generally use air temperature, photoperiod, and chilling units in different configurations and combinations to parameterize the response of plants to bioclimatic controls and predict the timing of phenophase transitions (Basler, 2016; Hufkens et al., 2018). However, as we described previously, Clark et al. (2014a, 2014b) argue that most conventional phenology models are fundamentally limited because: (1) they aggregate measurements with substantial day-to-day variability over periods of weeks-to-months into single parameters and therefore do not capture how short-term variability in control variables influences the timing of leaf emergence; (2) they rely on parameters that are not identifiable; and (3) they do not account for uncertainty in model predictors or leaf emergence data. As a solution, Hänninen et al. (2019) argue that carefully designed factorial experiments provide the most robust basis for improving understanding of processes that control leaf emergence, and hence, for developing and testing process-based models. However, implementing such studies is difficult and expensive, and collecting sufficient sample data to support robust and generalizable models is generally not possible. Reflecting these challenges, results from a meta-analysis of warming studies showed that phenological changes observed in such experiments do not replicate the magnitude of phenological responses to natural variation in air temperature observed in natural systems (Wolkovich et al., 2012).

Data-driven models like the CDSOM are not a panacea, but they do resolve several of the issues discussed above. In addition to addressing the three limitations identified by Clark et al. (2014a, 2014b), functional relationships among control variables in CDSOM are entirely estimated from data. Hence the CDSOM avoids issues related to misspecification of functional relationships that are inherent to conventional models. Further, by exploiting time series of remote sensing observations collected over large areas that span nearly two decades, the CDSOM results presented here capture and reflect a much broader range of climate regimes and climate variability than is generally possible using designed experiments. Indeed, we posit that natural variability captured through interannual variability in climate over large geographic scales provides an important and useful strategy for characterizing and understanding the sensitivity of plant phenology to climate change (Friedl

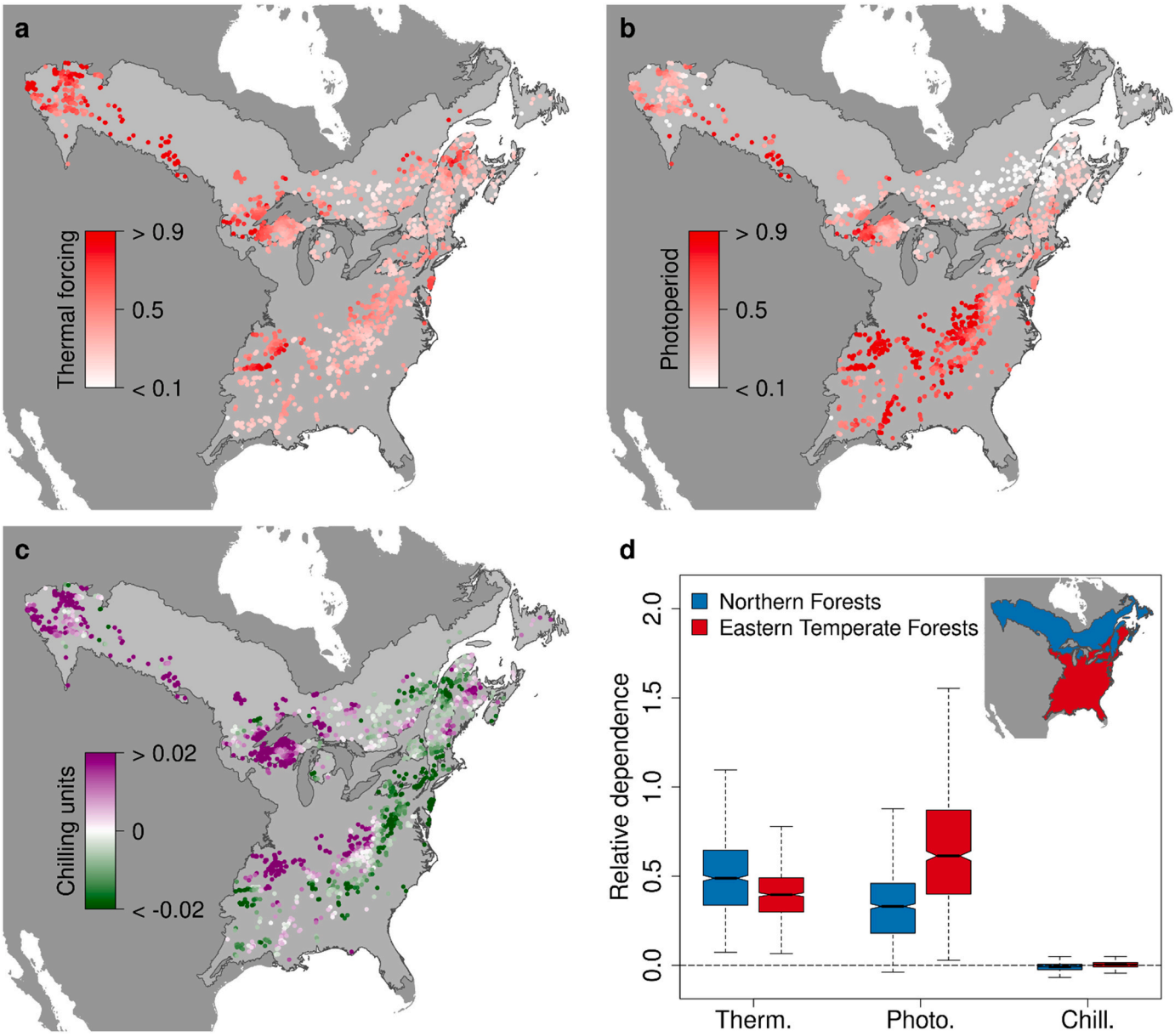

Fig. 4. Geographic variation in the dependence of spring greenup onset date to: (a) thermal forcing, (b) photoperiod, and (c) chilling units. In panel (d), boxplots show the distribution of model coefficients for each control variable during the pre-season period prior to leaf emergence in Northern Forests (blue) versus Eastern Temperate Forests (red). Differences between the means in both cases are statistically significant ($p < 0.001$). (For interpretation of the references to colour in this figure legend, the reader is referred to the web version of this article.)

et al., 2014).

Moreover, and perhaps most importantly, while the patterns presented in Figs. 4-7 are superficially consistent with results from previous studies suggesting that the timing of spring greenup in deciduous forests has become less sensitive to thermal forcing and that the so-called 'temperature sensitive period' of temperate and boreal trees is changing (Fu et al., 2019, 2015; Piao et al., 2017). We suggest that this inference may be spurious. Specifically, results from the CDSOM show that thermal forcing control on the timing of greenup is heterogeneous and exhibits weak covariance with pre-season period. Hence, apparent decreases in temperature sensitivity actually reflect shorter pre-season periods with increased photoperiod control (Keenan et al., 2019). Stated another way, as the climate warms, higher temperatures tend to increase the relative importance of photoperiod, while dependence on temperature has remained relatively constant. Further, in regions where mean annual temperature is below ~10 °C, which encompasses a significant proportion of the temperate zone and all of the boreal zone, photoperiod control is modest and thermal forcing is clearly the dominant control. Indeed, our results suggest that the biogeographic range in which the relative importance of photoperiod control is increasing is restricted to locations with mean annual temperatures between ~8–10 °C, and hence, is relatively narrow.

The simplest explanation for why photoperiod control varies geographically is provided by the "law of the minimum", which states that plant growth is controlled by the scarcest resource rather than by the total resources available (Liebig, 1841). Our results are, to a first order, consistent with this law. In cold regions (i.e., identified here as regions where mean annual temperature is less than ~10 °C; Fig. 5), temperature is the primary limiting factor that controls the timing of greenup. In warmer regions where temperature is less limiting, light (or moisture) becomes the primary limiting resource. Invoking a similar argument, Park et al. (2019) suggest that extensive areas of high-latitude

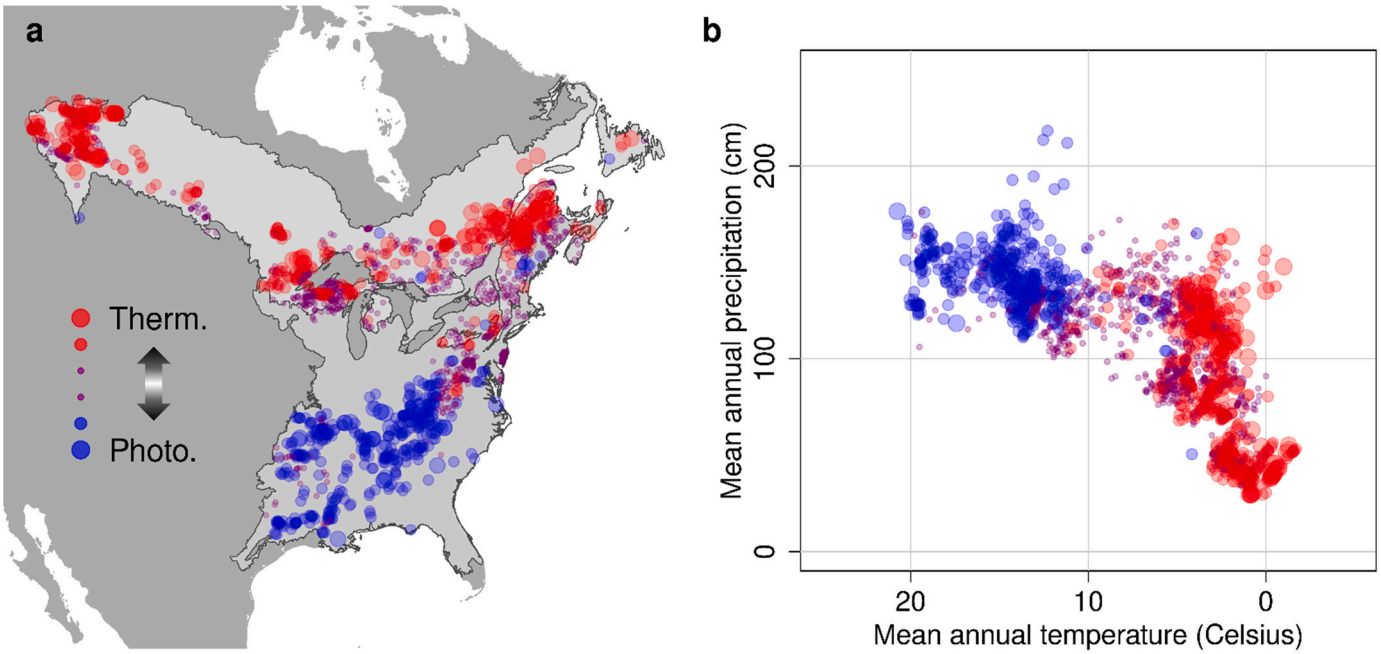

Fig. 5. Relative importance (*RI*) of thermal forcing versus photoperiod. Circles in red and blue show locations where thermal forcing and photoperiod, respectively, exert stronger control on the timing of spring greenup; purple circles identify locations where the magnitude of thermal forcing and photoperiod are roughly equivalent. The size of each circle is proportional to the magnitude of *RI* in each cell. (For interpretation of the references to colour in this figure legend, the reader is referred to the web version of this article.)

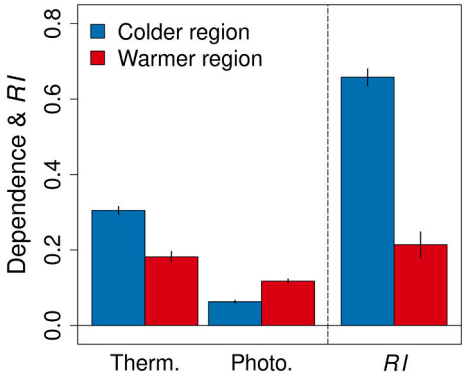

Fig. 6. Dependence of cloned lilac leaf unfolding date on thermal forcing and photoperiod, and relative importance (*RI*). 254 total leaf unfolding dates from cloned lilac were divided into two groups based on mean annual temperature (≤ 10 °C, $n = 182$; > 10 °C, $n = 72$). The left panel plots the mean dependence of leaf unfolding on thermal forcing and photoperiod estimated by the CDSOM. The right panel plots the mean *RI* in each group. Positive *RI* indicates stronger control by thermal forcing relative to photoperiod. Vertical lines show ± 1 standard deviation.

ecosystems that were previously constrained by temperature are becoming more sensitive to photoperiod. Further, the results from our study are consistent with recent experimental results from Zohner et al. (2016), who concluded that springtime phenology in deciduous trees at lower latitudes tended to depend more strongly on photoperiod, while species at high latitudes leafed out independent of photoperiod. Hence our results are consistent with both long-established and more recent ecological literature.

Lastly, it is important to note several limitations of the current study. First, rather than modeling the role of chilling in controlling spring greenup using continuous (i.e., daily) forcing (Hänninen et al., 2019; Murray et al., 1989), the CDSOM uses chilling units, which provide an accumulated measure chilling requirements. This suggests that the role of the chilling units may not be fully accounted for in this study, and may explain the relatively minor role of chilling units in predicting the timing of spring greenup that we observed in this study (Fig. 4c and d) (c.f., Heide and Prestrud, 2005; Laube et al., 2014). Second, to capture the effect of thermal forcing, the CDSOM used daily mean temperature as opposed to other measures of thermal forcing such as daily maximum and minimum temperature, which some studies have suggested may be better predictors. However, results from CDSOM using daily maximum and minimum temperatures as inputs did not show significant differences from results based on daily mean temperatures (not shown), and more generally, results from studies that have explored this question are somewhat inconsistent (c.f., Huang et al., 2020; Piao et al., 2015; Shen et al., 2018). That said, because continuous development models are explicitly designed to capture the effects of short-term variability in forcing variables, selection of optimal metrics to this variability is clearly important and merits more investigation.

5. Conclusions

Changes in springtime phenology are among the most obvious and observable responses of organisms to climate change, but the mechanisms behind these changes are poorly understood (Parmesan and Yohe, 2003; Piao et al., 2019). By directly estimating and mapping the geographic dependence of greenup on photoperiod and thermal forcing, results from this study elucidate how the nature and magnitude bioclimatic control on spring phenology depend on geography and climate, and provide a novel and nuanced explanation for why the temperature sensitivity of deciduous forests appears to be decreasing. Specifically, our results indicate that apparent changes in temperature sensitivity may reflect a misinterpretation of the data, and where present, observed decreases actually reflect increased dependence on photoperiod. The results also help to clarify the mechanisms behind observed changes and have important implications for a variety of ecological processes, such as the role of safety mechanisms that are widely ascribed to photoperiod constraints on spring phenology (Körner and Basler, 2010). For example, Fig. 5 shows that the relative importance of photoperiod decreases as

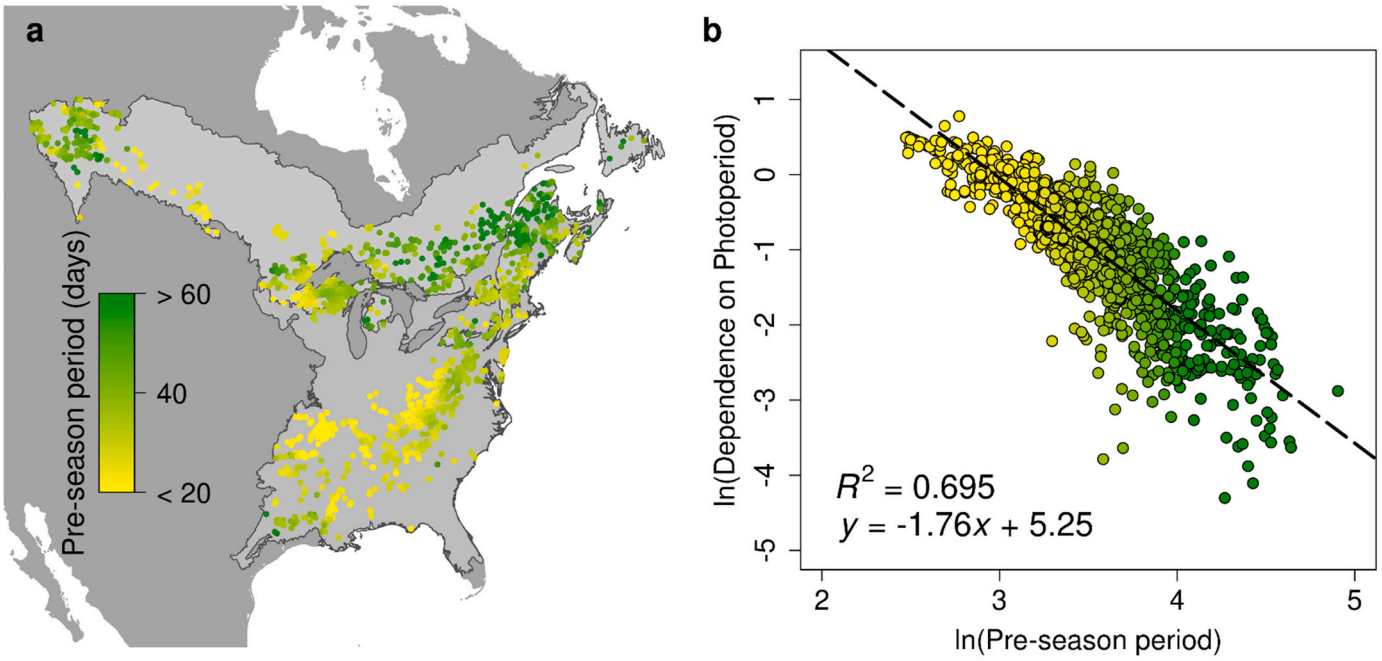

Fig. 7. Variation in pre-season period and the relationship between greenup dependence on photoperiod and length of pre-season period. (a) Geographic pattern in pre-season period, and (b) log-log relationship between the dependence of greenup on photoperiod and the length of the pre-season period.

mean annual temperature decreases, which suggests that safety mechanisms related to photoperiod provide only modest protection in colder climates (Richardson et al., 2018a). More generally, our results support the argument posited by Zohner et al. (2016) who reported that tree species with strong photoperiod control on leaf-out tend to be located in warmer regions, and challenge the idea that photoperiod provides a safeguard against early leaf emergence in temperate woody species.

Author contributions

M.M. and M.A.F designed the analysis and led the drafting of the manuscript. M.M. and B.S. developed the model. MM. performed the analysis. B.S. and A.D.R. contributed analysis ideas and participated in drafting the manuscript.

Declaration of Competing Interest

The authors declare no competing interests.

Acknowledgements

This research was funded by the MacroSystems Biology Program of National Science Foundation (Grant numbers EF 1702627 and 1702697). ADR acknowledges support from NSF's (US National Science Foundation) LTER program through DEB-1637685 and and DEB-1832210.

Appendix A. Appendix

Table A1
Models descriptions.

Model	Model type	Variables	Main characteristics & Statistical assumptions of the model
CDSOM	Date-driven	h; δh; h_{max}; X; T; L; CU; β; P; κ; λ; Y; T_b	Phenological development responses continuously to variations in environmental controls at daily time step throughout pre-season period; Invoking no assumptions about functional relationships between control variables
TT	Knowledge-driven	F^*; S_f; T; T_b	Greenup onset occurs when accumulated forcing reaches a critical threshold, which sorely relies only on thermal forcing with no additional factors
PTT	Knowledge-driven	F^*; S_f; T; T_b; L	Greenup onset occurs when accumulated forcing reaches a critical threshold, but the rate of thermal forcing is regulated by photoperiod
M1	Knowledge-driven	F^*; S_f; T; T_b; L; k	Greenup onset occurs when accumulated forcing reaches a critical threshold, but the rate of thermal forcing is regulated by photoperiod as an exponential
AT	Knowledge-driven	F^*; NCD; a; b; c	Greenup onset occurs when accumulated forcing reaches a critical threshold, but the rate of thermal forcing is regulated by the number of chilling days

CDSOM: Continuous Development Spring Onset Model; TT: Thermal Time model (TT); PTT: Photo-Thermal Time model (PTT); M1: Exponential Photo-Thermal Time model (M1); AT: Alternating model; h: latent state; δh: daily latent state increment; h_{max}: theoretical final state of h; X: matrix of predictor variables T, L, and CU (daily mean temperature, day-length, and chilling units, respectively); β: vector of estimated model coefficient for T, L, and CU; P: probability that greenup onset occurs; κ and λ: intercept and slope for logit transformation, respectively; Y: Bernoulli trial indicating whether or not greenup onset has occurred; T_b: base temperature for chilling requirement; F^*: critical threshold that spring greenup onset occurs when the state of forcing (S_f) reaches it; k: exponential coefficient for M1; NCD: number of chilling days; estimated constants for AT.

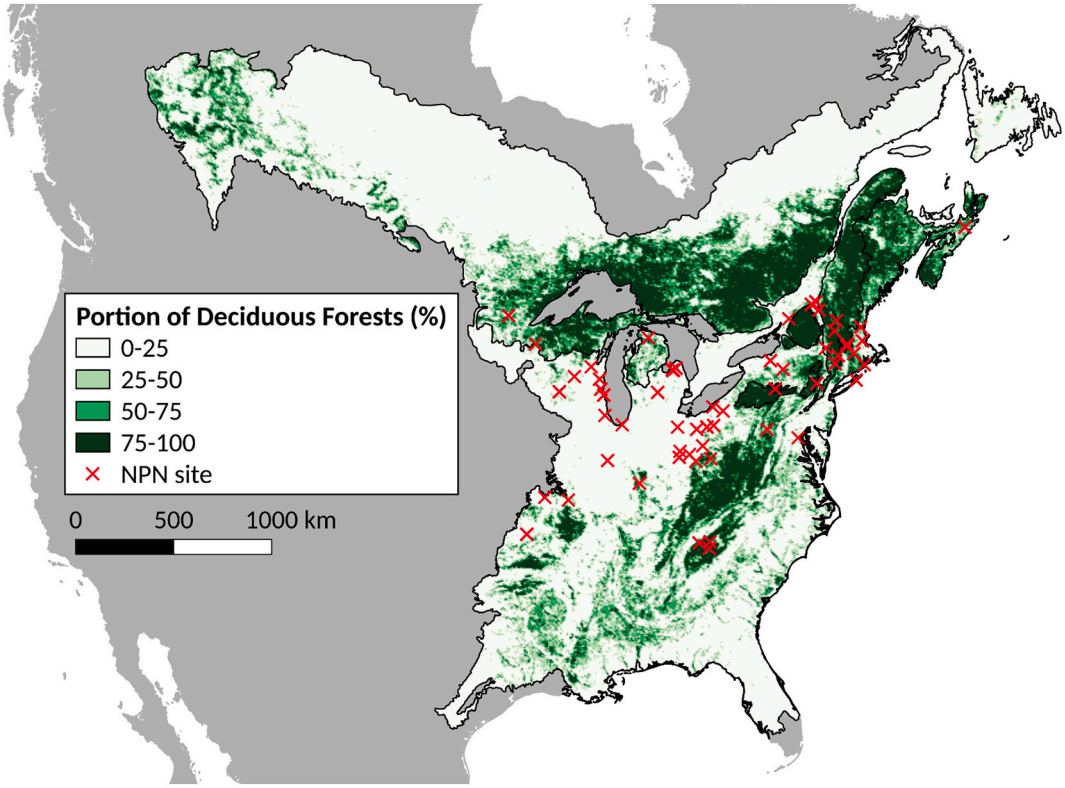

Fig. A1. Map of the study area. Extents of the US EPA Northern Forest and Eastern Temperate Forest Level I ecoregions, along with the proportion 500 m MODIS pixels labeled as deciduous forests in each grid cell according to the Collection 6 MODIS Land Cover Type product. Red crosses show the USA-National Phenology Network site locations where lilac data are collected. Note that because the MODIS Land Cover Type product uses a threshold of 60% cover to define forest classes, the map shown in Fig. A1 modestly over-represents the actual proportion of deciduous forest cover. (For interpretation of the references to colour in this figure legend, the reader is referred to the web version of this article.)

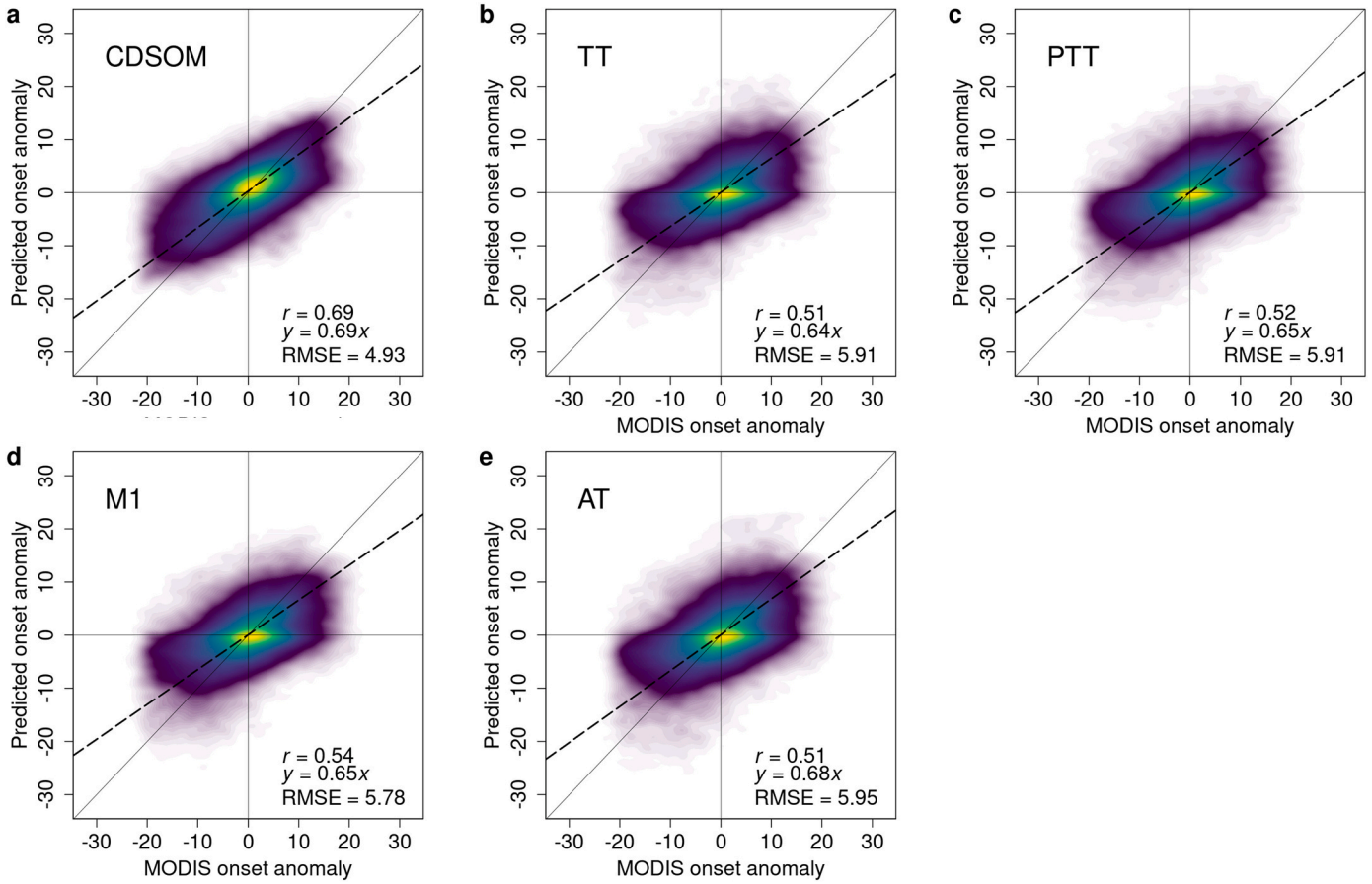

Fig. A2. Relationship between anomalies in MODIS onset dates and anomalies in model-predicted onset dates. Panels (a)-(e) show results for the Continuous Development Spring Onset Model (CDSOM), the thermal time model (TT), the photo-thermal time model (PTT), the exponential photo-thermal time model (M1), and the alternating model (AT), respectively. Dashed lines and correlation coefficients (r) show the results from standard major axis regression.

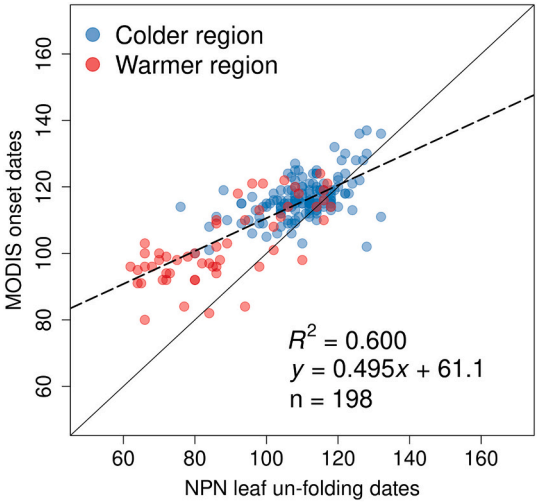

Fig. A3. Relationship between MODIS greenup dates and leaf unfolding dates from the USA-NPN cloned lilac dataset. The colder (blue dots) and warmer (red dots) sites are divided based on mean annual temperature (i.e., colder $\leq$10 °C; warmer >10 °C). n (= 198) is different from the total number of USA-NPN leaf unfolding dates (n = 254) due to cases where no MODIS dates were available because the lilac site was not located in a location dominated by deciduous or mixed forest at the scale of MODIS pixels. (For interpretation of the references to colour in this figure legend, the reader is referred to the web version of this article.)

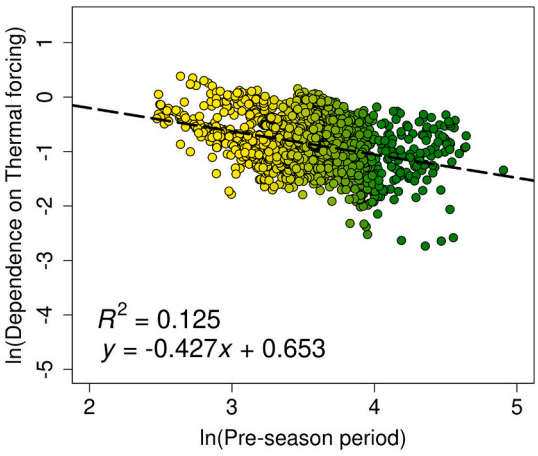

Fig. A4. Relationship between pre-season period length and dependence on thermal forcing.

References

Abercrombie, S.P., Friedl, M.A., 2016. Improving the consistency of multitemporal land cover maps using a hidden Markov model. IEEE Trans. Geosci. Remote Sens. 54, 703–713. https://doi.org/10.1109/TGRS.2015.2463689.

Basler, D., 2016. Evaluating phenological models for the prediction of leaf-out dates in six temperate tree species across Central Europe. Agric. For. Meteorol. 217, 10–21. https://doi.org/10.1016/j.agrformet.2015.11.007.

Basler, D., Körner, C., 2012. Photoperiod sensitivity of bud burst in 14 temperate forest tree species. Agric. For. Meteorol. 165, 73–81. https://doi.org/10.1016/j.agrformet.2012.06.001.

Blümel, K., Chmielewski, F.-M., 2012. Shortcomings of classical phenological forcing models and a way to overcome them. Agric. For. Meteorol. 164, 10–19. https://doi.org/10.1016/j.agrformet.2012.05.001.

Bolton, D.K., Gray, J.M., Melaas, E.K., Moon, M., Eklundh, L., Friedl, M.A., 2020. Continental-scale land surface phenology from harmonized Landsat 8 and Sentinel-2 imagery. Remote Sens. Environ. 240, 111685. https://doi.org/10.1016/j.rse.2020.111685.

Cannell, M.G.R., Smith, R.I., 1983. Thermal time, chill days and prediction of budburst in Picea sitchensis. J. Appl. Ecol. 20, 951–963. https://doi.org/10.2307/2403139.

Chuine, I., Régnière, J., 2017. Process-based models of phenology for plants and animals. Annu. Rev. Ecol. Evol. Syst. 48, 159–182. https://doi.org/10.1146/annurev-ecolsys-110316-022706.

Chuine, I., Cour, P., Rousseau, D.D., 1999. Selecting models to predict the timing of flowering of temperate trees: implications for tree phenology modelling. Plant Cell Environ. 22, 1–13. https://doi.org/10.1046/j.1365-3040.1999.00395.x.

Chuine, I., Bonhomme, M., Legave, J.-M., García de Cortázar-Atauri, I., Charrier, G., Lacointe, A., Améglio, T., 2016. Can phenological models predict tree phenology accurately in the future? The unrevealed hurdle of endodormancy break. Glob. Chang. Biol. 22, 3444–3460. https://doi.org/10.1111/gcb.13383.

Clark, J.S., Melillo, J., Mohan, J., Salk, C., 2014a. The seasonal timing of warming that controls onset of the growing season. Glob. Chang. Biol. 20, 1136–1145. https://doi.org/10.1111/gcb.12420.

Clark, J.S., Salk, C., Melillo, J., Mohan, J., 2014b. Tree phenology responses to winter chilling, spring warming, at north and south range limits. Funct. Ecol. 28, 1344–1355. https://doi.org/10.1111/1365-2435.12309.

Črepinšek, Z., Kajfež-Bogataj, L., Bergant, K., 2006. Modelling of weather variability effect on fitophenology. Ecol. Modell., Special Issue on the Fourth Eur. Conf. on Ecol. Modell. 194, 256–265. https://doi.org/10.1016/j.ecolmodel.2005.10.020.

Friedl, M.A., Gray, J.M., Melaas, E.K., Richardson, A.D., Hufkens, K., Keenan, T.F., Bailey, Amey, O'Keefe, J., 2014. A tale of two springs: using recent climate anomalies to characterize the sensitivity of temperate forest phenology to climate change. Environ. Res. Lett. 9, 054006 https://doi.org/10.1088/1748-9326/9/5/054006.

Fu, Y.H., Zhao, H., Piao, S., Peaucelle, M., Peng, S., Zhou, G., Ciais, P., Huang, M., Menzel, A., Peñuelas, J., Song, Y., Vitasse, Y., Zeng, Z., Janssens, I.A., 2015. Declining global warming effects on the phenology of spring leaf unfolding. Nature 526, 104–107. https://doi.org/10.1038/nature15402.

Fu, Y.H., Geng, X., Hao, F., Vitasse, Y., Zohner, C.M., Zhang, X., Zhou, X., Yin, G., Peñuelas, J., Piao, S., Janssens, I.A., 2019. Shortened temperature-relevant period of spring leaf-out in temperate-zone trees. Glob. Chang. Biol. 25, 4282–4290. https://doi.org/10.1111/gcb.14782.

Gray, J., Sulla-Menashe, D., Friedl, M.A., 2019. User Guide to Collection 6 MODIS Land Cover Dynamics (MCD12Q2) Product. https://doi.org/10.5067/MODIS/MCD12Q2.006.

Güsewell, S., Furrer, R., Gehrig, R., Pietragalla, B., 2017. Changes in temperature sensitivity of spring phenology with recent climate warming in Switzerland are related to shifts of the preseason. Glob. Chang. Biol. 23, 5189–5202. https://doi.org/10.1111/gcb.13781.

Hänninen, H., Kramer, K., Tanino, K., Zhang, R., Wu, J., Fu, Y.H., 2019. Experiments are necessary in process-based tree phenology Modelling. Trends Plant Sci. 24, 199–209. https://doi.org/10.1016/j.tplants.2018.11.006.

Heide, O.M., Prestrud, A.K., 2005. Low temperature, but not photoperiod, controls growth cessation and dormancy induction and release in apple and pear. Tree Physiol. 25, 109–114. https://doi.org/10.1093/treephys/25.1.109.

Huang, Y., Jiang, N., Shen, M., Guo, L., 2020. Effect of preseason diurnal temperature range on the start of vegetation growing season in the northern hemisphere. Ecol. Indic. 112, 106161. https://doi.org/10.1016/j.ecolind.2020.106161.

Hufkens, K., Basler, D., Milliman, T., Melaas, E.K., Richardson, A.D., 2018. An integrated phenology modelling framework in r. Methods Ecol. Evol. 9, 1276–1285. https://doi.org/10.1111/2041-210X.12970.

Hunter, A.F., Lechowicz, M.J., 1992. Predicting the timing of budburst in temperate trees. J. Appl. Ecol. 29, 597–604. https://doi.org/10.2307/2404467.

Jackson, S.D., 2009. Plant responses to photoperiod. New Phytol. 181, 517–531. https://doi.org/10.1111/j.1469-8137.2008.02681.x.

Keenan, T.F., Gray, J., Friedl, M.A., Toomey, M., Bohrer, G., Hollinger, D.Y., Munger, J. W., O'Keefe, J., Schmid, H.P., Wing, I.S., Yang, B., Richardson, A.D., 2014. Net carbon uptake has increased through warming-induced changes in temperate forest phenology. Nat. Clim. Chang. 4, 598–604. https://doi.org/10.1038/nclimate2253.

Keenan, T.F., Richardson, A.D., Hufkens, K., 2019. On quantifying the apparent temperature sensitivity of plant phenology. New Phytol nph 16114. https://doi.org/10.1111/nph.16114.

Körner, C., Basler, D., 2010. Phenology under global warming. Science 327, 1461–1462. https://doi.org/10.1126/science.1186473.

Laube, J., Sparks, T.H., Estrella, N., Höfler, J., Ankerst, D.P., Menzel, A., 2014. Chilling outweighs photoperiod in preventing precocious spring development. Glob. Chang. Biol. 20, 170–182. https://doi.org/10.1111/gcb.12360.

Liebig, J., 1841. Organic chemistry in its applications to agriculture and physiology. J. Owen. Taylor and Walton, London.

Liu, Q., Fu, Y.H., Liu, Y., Janssens, I.A., Piao, S., 2017. Simulating the onset of spring vegetation growth across the northern hemisphere. Glob. Chang. Biol. 24, 1342–1356. https://doi.org/10.1111/gcb.13954.

Masle, J., Doussinault, G., Farquhar, G.D., Sun, B., 1989. Foliar stage in wheat correlates better to photothermal time than to thermal time. Plant Cell Environ. 12, 235–247. https://doi.org/10.1111/j.1365-3040.1989.tb01938.x.

Melaas, E.K., Richardson, A.D., Friedl, M.A., Dragoni, D., Gough, C.M., Herbst, M., Montagnani, L., Moors, E., 2013. Using FLUXNET data to improve models of springtime vegetation activity onset in forest ecosystems. Agric. For. Meteorol. 171–172, 46–56. https://doi.org/10.1016/j.agrformet.2012.11.018.

Melaas, E.K., Sulla-Menashe, D., Friedl, M.A., 2018. Multidecadal changes and interannual variation in springtime phenology of north American temperate and boreal deciduous forests. Geophys. Res. Lett. 45, 2679–2687. https://doi.org/10.1002/2017GL076933.

Menzel, A., Sparks, T.H., Estrella, N., Koch, E., Aasa, A., Ahas, R., Alm-Kübler, K., Bissolli, P., Braslavská, O., Briede, A., Chmielewski, F.M., Crepinsek, Z., Curnel, Y., Dahl, Å., Defila, C., Donnelly, A., Filella, Y., Jatczak, K., Måge, F., Mestre, A., Nordli, Ø., Peñuelas, J., Pirinen, P., Remišová, V., Scheifinger, H., Striz, M., Susnik, A., Vliet, A.J.H.V., Wielgolaski, F.-E., Zach, S., Zust, A., 2006. European phenological response to climate change matches the warming pattern. Glob. Chang. Biol. 12, 1969–1976. https://doi.org/10.1111/j.1365-2486.2006.01193.x.

Migliavacca, M., Sonnentag, O., Keenan, T.F., Cescatti, A., O&apos, Keefe, J., Richardson, A.D., 2012. On the uncertainty of phenological responses to climate change, and implications for a terrestrial biosphere model. Biogeosciences 9, 2063–2083. https://doi.org/10.5194/bg-9-2063-2012.

Montgomery, R.A., Rice, K.E., Stefanski, A., Rich, R.L., Reich, P.B., 2020. Phenological responses of temperate and boreal trees to warming depend on ambient spring temperatures, leaf habit, and geographic range. Proc. Natl. Acad. Sci. U. S. A. 201917508 https://doi.org/10.1073/pnas.1917508117.

Moon, M., Zhang, X., Henebry, G.M., Liu, L., Gray, J.M., Melaas, E.K., Friedl, M.A., 2019. Long-term continuity in land surface phenology measurements: a comparative assessment of the MODIS land cover dynamics and VIIRS land surface phenology products. Remote Sens. Environ. 226, 74–92. https://doi.org/10.1016/j.rse.2019.03.034.

Moon, M., Li, D., Liao, W., Rigden, A.J., Friedl, M.A., 2020. Modification of surface energy balance during springtime: the relative importance of biophysical and meteorological changes. Agric. For. Meteorol. 284, 107905. https://doi.org/10.1016/j.agrformet.2020.107905.

Murray, M.B., Cannell, M.G.R., Smith, R.I., 1989. Date of budburst of fifteen tree species in Britain following climatic warming. J. Appl. Ecol. 26, 693–700. https://doi.org/10.2307/2404093.

Park, T., Chen, C., Macias-Fauria, M., Tømmervik, H., Choi, S., Winkler, A., Bhatt, U.S., Walker, D.A., Piao, S., Brovkin, V., Nemani, R.R., Myneni, R.B., 2019. Changes in timing of seasonal peak photosynthetic activity in northern ecosystems. Glob Change Biol gcb 14638. https://doi.org/10.1111/gcb.14638.

Parmesan, C., Yohe, G., 2003. A globally coherent fingerprint of climate change impacts across natural systems. Nature 421, 37–42. https://doi.org/10.1038/nature01286.

Peñuelas, J., Rutishauser, T., Filella, I., 2009. Phenology feedbacks on climate change. Science 324, 887–888. https://doi.org/10.1126/science.1173004.

Piao, S., Tan, J., Chen, A., Fu, Y.H., Ciais, P., Liu, Q., Janssens, I.A., Vicca, S., Zeng, Z., Jeong, S.-J., Li, Y., Myneni, R.B., Peng, S., Shen, M., Peñuelas, J., 2015. Leaf onset in the northern hemisphere triggered by daytime temperature. Nat. Commun. 6, 6911. https://doi.org/10.1038/ncomms7911.

Piao, S., Liu, Z., Wang, T., Peng, S., Ciais, P., Huang, M., Ahlstrom, A., Burkhart, J.F., Chevallier, F., Janssens, I.A., Jeong, S.-J., Lin, X., Mao, J., Miller, J., Mohammat, A., Myneni, R.B., Peñuelas, J., Shi, X., Stohl, A., Yao, Y., Zhu, Z., Tans, P.P., 2017. Weakening temperature control on the interannual variations of spring carbon uptake across northern lands. Nat. Clim. Chang. 7, 359–363. https://doi.org/10.1038/nclimate3277.

Piao, S., Liu, Q., Chen, A., Janssens, I.A., Fu, Y., Dai, J., Liu, L., Lian, X., Shen, M., Zhu, X., 2019. Plant phenology and global climate change: current progresses and challenges. Glob. Chang. Biol. https://doi.org/10.1111/gcb.14619.

Qiu, T., Song, C., Clark, J.S., Seyednasrollah, B., Rathnayaka, N., Li, J., 2020. Understanding the continuous phenological development at daily time step with a Bayesian hierarchical space-time model: impacts of climate change and extreme weather events. Remote Sens. Environ. 247, 111956. https://doi.org/10.1016/j.rse.2020.111956.

Richardson, A.D., Keenan, T.F., Migliavacca, M., Ryu, Y., Sonnentag, O., Toomey, M., 2013. Climate change, phenology, and phenological control of vegetation feedbacks to the climate system. Agric. For. Meteorol. 169, 156–173. https://doi.org/10.1016/j.agrformet.2012.09.012.

Richardson, A.D., Hufkens, K., Milliman, T., Aubrecht, D.M., Furze, M.E., Seyednasrollah, B., Krassovski, M.B., Latimer, J.M., Nettles, W.R., Heiderman, R.R., Warren, J.M., Hanson, P.J., 2018a. Ecosystem warming extends vegetation activity but heightens vulnerability to cold temperatures. Nature. https://doi.org/10.1038/s41586-018-0399-1.

Richardson, A.D., Hufkens, K., Milliman, T., Frolking, S., 2018b. Intercomparison of phenological transition dates derived from the PhenoCam dataset V1.0 and MODIS satellite remote sensing. Sci. Rep. 8, 5679. https://doi.org/10.1038/s41598-018-23804-6.

Rosemartin, A.H., Denny, E.G., Weltzin, J.F., Lee Marsh, R., Wilson, B.E., Mehdipoor, H., Zurita-Milla, R., Schwartz, M.D., 2015. Lilac and honeysuckle phenology data 1956–2014. Scientific Data 2, 150038. https://doi.org/10.1038/sdata.2015.38.

Schewe, J., Gosling, S.N., Reyer, C., Zhao, F., Ciais, P., Elliott, J., Francois, L., Huber, V., Lotze, H.K., Seneviratne, S.I., van Vliet, M.T.H., Vautard, R., Wada, Y., Breuer, L., Büchner, M., Carozza, D.A., Chang, J., Coll, M., Deryng, D., de Wit, A., Eddy, T.D., Folberth, C., Frieler, K., Friend, A.D., Gerten, D., Gudmundsson, L., Hanasaki, N., Ito, A., Khabarov, N., Kim, H., Lawrence, P., Morfopoulos, C., Müller, C., Müller Schmied, H., Orth, R., Ostberg, S., Pokhrel, Y., Pugh, T.A.M., Sakurai, G., Satoh, Y., Schmid, E., Stacke, T., Steenbeek, J., Steinkamp, J., Tang, Q., Tian, H., Tittensor, D. P., Volkholz, J., Wang, X., Warszawski, L., 2019. State-of-the-art global models underestimate impacts from climate extremes. Nat. Commun. 10, 1005. https://doi.org/10.1038/s41467-019-08745-6.

Schwartz, M.D., Ahas, R., Aasa, A., 2006. Onset of spring starting earlier across the Northern hemisphere. Glob. Chang. Biol. 12, 343–351. https://doi.org/10.1111/j.1365-2486.2005.01097.x.

Senf, C., Pflugmacher, D., Heurich, M., Krueger, T., 2017. A Bayesian hierarchical model for estimating spatial and temporal variation in vegetation phenology from Landsat time series. Remote Sens. Environ. 194, 155–160. https://doi.org/10.1016/j.rse.2017.03.020.

Seyednasrollah, B., Swenson, J.J., Domec, J.-C., Clark, J.S., 2018. Leaf phenology paradox: why warming matters most where it is already warm. Remote Sens. Environ. 209, 446–455. https://doi.org/10.1016/j.rse.2018.02.059.

Seyednasrollah, B., Young, A.M., Li, X., Milliman, T., Ault, T., Frolking, S., Friedl, M., Richardson, A.D., 2020. Sensitivity of deciduous Forest phenology to environmental drivers: implications for climate change impacts across North America. Geophys. Res. Lett. 47 https://doi.org/10.1029/2019GL086788.

Shen, X., Liu, B., Henderson, M., Wang, L., Wu, Z., Wu, H., Jiang, M., Lu, X., 2018. Asymmetric effects of daytime and nighttime warming on spring phenology in the temperate grasslands of China. Agric. For. Meteorol. 259, 240–249. https://doi.org/10.1016/j.agrformet.2018.05.006.

Su, Y.-S., Yajima, M., 2015. R2jags: Using R to Run "JAGS".

Sulla-Menashe, D., Gray, J.M., Abercrombie, S.P., Friedl, M.A., 2019. Hierarchical mapping of annual global land cover 2001 to present: the MODIS collection 6 land cover product. Remote Sens. Environ. 222, 183–194. https://doi.org/10.1016/j.rse.2018.12.013.

Thornton, P.E., Thornton, M.M., Mayer, B.W., Wei, Y., Devarakonda, R., Vose, R.S., Cook, R.B., 2017. Daymet: Daily Surface Weather Data on a 1-Km Grid for North America, Version 3. https://doi.org/10.3334/ORNLDAAC/1328.

Walther, G.-R., Post, E., Convey, P., Menzel, A., Parmesan, C., Beebee, T.J.C., Fromentin, J.-M., Hoegh-Guldberg, O., Bairlein, F., 2002. Ecological responses to recent climate change. Nature 416, 389–395. https://doi.org/10.1038/416389a.

Wenden, B., Mariadassou, M., Chmielewski, F.-M., Vitasse, Y., 2020. Shifts in the temperature-sensitive periods for spring phenology in European beech and pedunculate oak clones across latitudes and over recent decades. Glob. Chang. Biol. 26, 1808–1819. https://doi.org/10.1111/gcb.14918.

Wolkovich, E.M., Cook, B.I., Allen, J.M., Crimmins, T.M., Betancourt, J.L., Travers, S.E., Pau, S., Regetz, J., Davies, T.J., Kraft, N.J.B., Ault, T.R., Bolmgren, K., Mazer, S.J., McCabe, G.J., McGill, B.J., Parmesan, C., Salamin, N., Schwartz, M.D., Cleland, E.E., 2012. Warming experiments underpredict plant phenological responses to climate change. Nature 485, 494–497. https://doi.org/10.1038/nature11014.

Zhang, X., Liu, L., Liu, Y., Jayavelu, S., Wang, J., Moon, M., Henebry, G.M., Friedl, M.A., Schaaf, C.B., 2018. Generation and evaluation of the VIIRS land surface phenology product. Remote Sens. Environ. 216, 212–229. https://doi.org/10.1016/j.rse.2018.06.047.

Zohner, C.M., Benito, B.M., Svenning, J.-C., Renner, S.S., 2016. Day length unlikely to constrain climate-driven shifts in leaf-out times of northern woody plants. Nat. Clim. Chang. 6, 1120–1123. https://doi.org/10.1038/nclimate3138.